ARTICLE NO. 80-4127

Optimal Large-Angle Single-Axis Rotational Maneuvers of Flexible Spacecraft

James D. Turner* and John L. Junkins†
Virginia Polytechnic Institute and State University, Blacksburg, Va.

The necessary conditions formulated from Pontryagin's principle for optimal single-axis reorientations of a flexible vehicle having a control system capable of generating a continuous torque (on a "rigid part" of the structure) are discussed in this paper. The flexural deformations are modeled using the "assumed modes" method and only small (linear) flexural displacements are considered. A single-stage relaxation process is proposed for solution of the two-point boundary-value problem. Starting iteratives for initial costate variables are obtained by zeroing the kinematic nonlinearity in the state equation, leading to a closed-form solution algorithm. The relaxation process increases the participation of the nonlinearity in a sequence of neighboring optimal solutions, converging finally to the solution of the nonlinear problem.

I. Introduction

A PROBLEM of current interest is the rotational and configuration control of flexible spacecraft. In particular, we consider here optimal large-angle rotational maneuvers with simultaneous vibration suppression. The motion is described by a system of hybrid coordinates, using a combination of discrete coordinates for translations and rotations of rigid bodies, and distributed or modal coordinates for the deformations of elastic bodies.[1,2]

In a recent paper by Junkins and Turner,[3] nonsingular, necessary conditions for optimal large-angle rotational maneuvers of rigid asymmetric vehicles were presented, and a relaxation procedure was demonstrated, which reliably solves the resulting two-point boundary-value problem. Also, prepared independently and in parallel with the present work, Breakwell[4] developed results which are essentially identical to the linearized version of the results herein. As a natural continuation of Ref. 3, the authors present here certain nonlinear extensions for the flexible body case.

The specific model considered in this paper (see Fig. 1) consists of a rigid hub with four identical elastic appendages attached symmetrically about the central hub. We consider only the case of a single-axis maneuver, with the flexible members restricted to displacements in the plane normal to the axis of rotation. We make the further assumption that the body, as a whole, experiences only antisymmetric modes of deformation (see Fig. 2).

The procedure used for analyzing the hybrid system is a discretization, whereby the displacement of the continuous elastic members is replaced by a finite series of known (admissible) space-dependent functions multiplied by time-dependent (to be determined) modal amplitudes.[3]

The necessary conditions for the optimal single-axis maneuver are presented in two parts. The first part (Secs. II-IV) consists of the formulation and solution of the linearized equations, while ignoring a to be specified kinematic nonlinearity (in order to obtain a closed-form solution algorithm for the unknown initial costates). The second part (Secs. V and VI) consists of presenting the general equations, including the effect of the kinematic nonlinearity. We also propose in Sec. VI a relaxation procedure (motivated by the success of the related process employed in Ref. 3) for solving the nonlinear two-point boundary-value problem which makes use of the initial costates determined in Sec. IV.A of this paper. In Sec. VII, we provide numerical results which support the validity and utility of these formulations.

Presented at the 2nd AIAA/VPI&SU Symposium on Dynamics and Control of Large Flexible Spacecraft, June 21-23, 1979; submitted Sept. 13, 1979; revision received Feb. 13, 1980.

Index category: Spacecraft Dynamics and Control.

*Dept. of Engineering Science and Mechanics; presently, Member of Technical Staff, Charles Stark Draper Labs., Cambridge, Mass. Member AIAA.

†Professor, Dept. of Engineering Science and Mechanics. Associate Fellow AIAA.

II. Equations of Motion

For the body being considered, the equations of motion can be obtained by Hamilton's extended principle.[5]

$$\int_{t_1}^{t_2} (\delta\mathcal{L} + \delta\mathcal{W})\,\mathrm{d}t = 0 \tag{1}$$

subject to

$$\delta\theta = \delta u = 0 \quad \text{at} \quad t_1, t_2$$

where $\mathcal{L} = \mathfrak{I} - \mathcal{V}$ is the system Lagrangian, $\delta\mathcal{W}$ represents the virtual work, $\delta\theta$ represents a virtual rotation, and δu represents a virtual elastic displacement.

The kinetic and potential energy expressions for the body (see Fig. 1) can be shown to be

$$\mathfrak{I} = \tfrac{1}{2}\dot{\theta}^2\left[\mathcal{J} + 4\int_A (u^2 - p^2)\,\mathrm{d}m\right] + 2\int_A \dot{u}^2\mathrm{d}m + 4\dot{\theta}\int_A x\dot{u}\mathrm{d}m \tag{2}$$

$$p^2 = \tfrac{1}{2}(L^2 - x^2)\left(\frac{\partial u}{\partial x}\right)^2$$

$$\mathcal{V} = 2\int_A EI\left[\frac{\partial^2 u}{\partial x^2}\right]^2 \mathrm{d}x \qquad (\dot{\ }) \equiv \frac{\mathrm{d}}{\mathrm{d}t}(\ ) \tag{3}$$

where $\mathcal{J}$ denotes the moment of inertia of the body about the spin axis in the undeformed state, the subscript A denotes that the integration is to be over one of the elastic appendages, and u denotes an elastic displacement. In Eqs. (2) and (3), we are only considering the elastic potential energy. We restrict attention to only these most dominant kinetic energy terms; all higher-order terms are neglected at the onset.

The virtual work in this example will just consist of the control torque generated to bring about the maneuver and hence $\delta\mathcal{W}$ has the form

$$\delta\mathcal{W} = U_T\delta\theta \qquad (U_T = \text{control torque}) \tag{4}$$

Before applying Hamilton's extended principle, we express, by the assumed modes method, the elastic displacements as

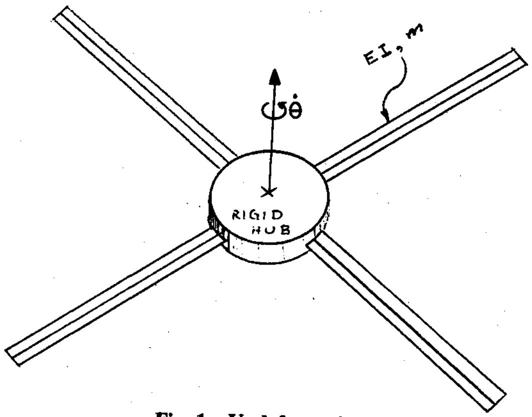

Fig. 1 Undeformed structure.

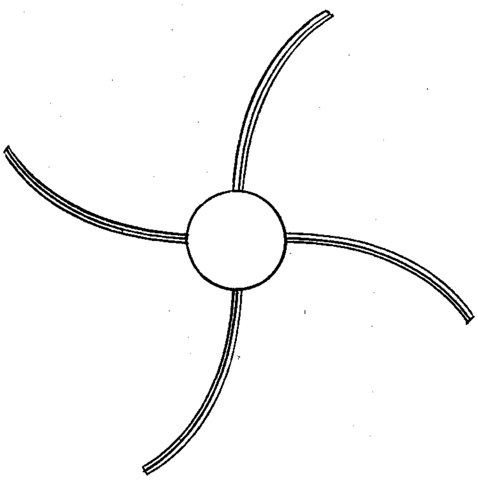

Fig. 2 Antisymmetric deformation.

the following series:

$$u(x,t) = \sum_{k=1}^{n} \eta_k(t)\phi_k(x) \tag{5}$$

where $\eta_k(t)$ represents the time-varying amplitudes, $\phi_k(x)$ represents an admissible assumed mode shape, and n represents the number of terms to be used in the approximation.

On introducing Eq. (5) into Eqs. (2) and (3), we obtain for the system Lagrangian

$$\mathcal{L} = \frac{\mathcal{I}}{2}\dot\theta^2 + \tfrac{1}{2}\dot\eta^T M_{\eta\eta}\dot\eta + \dot\theta M_{\theta\eta}^T\dot\eta + \tfrac{1}{2}\eta^T[\dot\theta^2(M_{\eta\eta}-M_p) - K_{\eta\eta}]\eta \tag{6}$$

where

$$\eta = [\eta_1, \eta_2, \ldots, \eta_n]^T$$

$$[M_{\eta\eta}]_{kl} = 4\int_A \phi_k\phi_l \mathrm{d}m \qquad (n\times n)$$

$$[M_p]_{kl} = 4\int_A \tfrac{1}{2}(L^2-x^2)\phi_k'\phi_l'\mathrm{d}m \qquad (n\times n)$$

$$[K_{\eta\eta}]_{kl} = 4\int_A EI\phi_k''\phi_l''\mathrm{d}x \qquad (n\times n)$$

$$[M_{\theta\eta}]_k = 4\int_A x\phi_k \mathrm{d}m \qquad (n\times 1)$$

L = appendage length

$$(\ )' \equiv \frac{\mathrm{d}}{\mathrm{d}x}(\ )$$

Substituting Eqs. (4) and (6) into Eq. (1) yields Lagrange's equations

$$\frac{\mathrm{d}}{\mathrm{d}t}\left(\frac{\partial\mathcal{L}}{\partial\dot\theta}\right) - \frac{\partial\mathcal{L}}{\partial\theta} = U_T \tag{7}$$

$$\frac{\mathrm{d}}{\mathrm{d}t}\left(\frac{\partial\mathcal{L}}{\partial\dot\eta}\right) - \frac{\partial\mathcal{L}}{\partial\eta} = 0 \tag{8}$$

From which the equajtions of motion follow as

$$\ddot\theta = (\mathcal{I} + \eta^T M_{\eta\eta}\eta)^{-1}[U_T - M_{\theta\eta}^T\ddot\eta - 2\dot\theta\dot\eta^T M_{\eta\eta}\eta] \tag{9}$$

$$M_{\eta\eta}\ddot\eta + [K_{\eta\eta} + \dot\theta^2\mathfrak{M}]\eta = -\ddot\theta M_{\theta\eta} \qquad \mathfrak{M} = M_p - M_{\eta\eta} \tag{10}$$

III. State Space Formulation

Since we have made the small deformation assumption, we can delete the quadratic deflection terms in Eq. (9). Since we are further ignoring the $\dot\theta^2$ term in Eq. (10) (for this part of the paper), Eqs. (9) and (10) can be cast in the linear matrix form

$$M\ddot\zeta + K\zeta = U_T[1 \ \ 0^T]^T \tag{11}$$

where

$$\zeta = \begin{Bmatrix} \theta \\ \hline \eta \end{Bmatrix} \quad M = \begin{bmatrix} \mathcal{I} & M_{\theta\eta}^T \\ M_{\theta\eta} & M_{\eta\eta} \end{bmatrix} \quad K = \begin{bmatrix} 0 & 0^T \\ 0 & K_{\eta\eta} \end{bmatrix}$$

and

$M = M^T$, a positive definite matrix

$K = K^T$, a positive semidefinite matrix (the null subspace corresponds to the rigid body mode)

In order to uncouple the equations in Eq. (11), we first solve the eigenvalue problem

$$\lambda_r^2 M\zeta_r = K\zeta_r \qquad (\lambda_r^2 = \text{eigenvalue}, \ \ \zeta_r = \text{eigenvector}) \tag{12}$$

to obtain the modal matrix $E = [\zeta_1, \zeta_2, \ldots, \zeta_n]$ subject to the normalizations

$$E^T M E = [I] \tag{13a}$$

with the consequence that

$$E^T K E = [\Delta^2] = \mathrm{diag}(\lambda_1^2, \lambda_2^2, \ldots, \lambda_n^2) \tag{13b}$$

On premultiplying Eq. (11) by E^T and introducing the coordinate transformation

$$\zeta = E\mathfrak{t} \tag{14}$$

and taking note of Eq. (13), the uncoupled matrix equation becomes

$$\ddot{\mathfrak{t}} + [\Delta^2]\mathfrak{t} = U_T V \tag{15}$$

where

$$V = E^T[1 \ \ 0^T]^T = [E_{11}, E_{12}, \ldots, E_{1N}]^T \qquad (N = n+1)$$

Defining the state variable subsets

$$s_1 = \mathfrak{t} \qquad s_2 = \dot{\mathfrak{t}} \tag{16}$$

leads to the first-order differential equations

$$\dot s_1 = s_2 \qquad \dot s_2 = -[\Delta^2]s_1 + U_T V \tag{17}$$

Letting $s = [s_1^T s_2^T]^T$, the state form of the differential equations becomes

$$\dot s = As + BU_T \tag{18}$$

where

$$A=\begin{bmatrix}[0] & [I]\\ -[\Delta^2] & [0]\end{bmatrix}\qquad B=\begin{Bmatrix}0'\\ V\end{Bmatrix}\qquad 0'=\begin{Bmatrix}0\\ 0\end{Bmatrix}$$

IV. Optimal Control Problem

A. Derivation of the Necessary Conditions from Pontryagin's Principle

Consider the rotational dynamics of a flexible space vehicle restricted to a single-axis maneuver where the dynamics are governed by Eq. (18). We seek a solution satisfying the prescribed terminal states

$$\zeta_0=[\theta_0 \quad \eta^T(0)]^T \qquad \dot{\zeta}_0=[\dot{\theta}_0 \quad \dot{\eta}^T(0)]^T \tag{19a}$$

and

$$\zeta_f=[\theta_f \quad \eta^T(t_f)]^T \qquad \dot{\zeta}_f=[\dot{\theta}_f \quad \dot{\eta}^T(t_f)]^T \tag{19b}$$

where we impose the requirement that $\eta(t_f)=\dot{\eta}(t_f)=0$ on the right-hand side of Eq. (19b) for the final time. In particular, we seek the torque history $U_T(t)$ generating an optimal solution of Eq. (18), initiating at Eq. (19a) and terminating at Eq. (19b) which minimizes the performance index

$$J=\tfrac{1}{2}\int_0^t [U_T W_{uu} U_T + s^T W_{ss} s]\,dt \tag{20}$$

where W_{uu} is a scalar weight on the control and W_{ss} is a weight matrix for the state variables. We restrict attention to a piecewise continuous torque history $U_T(t)$. The selection of the quadratic index, Eq. (20), has been made for convenience, recognizing that many other reasonable indices are possible,[6-10] and also recognizing that the choice of other than Eq. (20) may have significant impact, both on the computational problems and the resulting maneuvers.

In preparing to make use of Pontryagin's necessary conditions, we introduce the Hamiltonian function

$$\mathcal{H}=\tfrac{1}{2}(U_T W_{uu} U_T + s^T W_{ss} s)+\lambda^T(As+BU_T) \tag{21}$$

where the λ's are Lagrange multipliers (also known as costate or adjoint variables). In addition to Eq. (18), Pontryagin's principle requires as necessary conditions that λ satisfy costate differential equation derivable from

$$\dot{\lambda}=-\frac{\partial\mathcal{H}}{\partial s} \tag{22}$$

and that $U_T(t)$ must be chosen at every instant so that the Hamiltonian of Eq. (21) is minimized; thus for $U_T(t)$ continuous, we require

$$\frac{\partial\mathcal{H}}{\partial U_T}=0=W_{uu}U_T+B^T\lambda \tag{23}$$

from which the optimal torque is determined as a function of the costate variables as

$$U_T=-W_{uu}^{-1}B^T\lambda \tag{24}$$

The state and costate differential equations are summarized as:

State Equations (from substituting Eq. (24) into (18))

$$\dot{s}=As-BW_{uu}^{-1}B^T\lambda \tag{25a}$$

Costate Equations (obtained by carrying out implied operations in Eq. (22))

$$\dot{\lambda}=-W_{ss}s-A^T\lambda \tag{25b}$$

B. Solution for the Initial Costates

Thus, application of Pontryagin's principle has led, as usual, to a two-point boundary-value problem. The boundary conditions are known initially and finally for s, but not for λ. Observe, writing the merged state vector

$$X=[s^T \quad \lambda^T]^T \tag{26}$$

that Eq. (25) becomes

$$\dot{X}=\Omega X \tag{27}$$

where

$$\Omega=\begin{bmatrix}A & -BW_{uu}^{-1}B^T\\ -W_{ss} & -A^T\end{bmatrix}=\text{constant coefficient matrix}$$

Since Ω is constant, it is well-known that Eq. (27) possesses the solution

$$X(t)=\Phi(t,0)X(0) \tag{28}$$

where

$$\dot{\Phi}(t,0)=\Omega\Phi(t,0), \qquad \Phi(0,0)=[I] \tag{29}$$

and Φ is the $4N\times 4N$ state transition matrix.

Expanding Eq. (28), we obtain

$$\begin{Bmatrix}s(t_f)\\ \lambda(t_f)\end{Bmatrix}=\begin{bmatrix}\Phi_{ss} & \Phi_{s\lambda}\\ \Phi_{\lambda s} & \Phi_{\lambda\lambda}\end{bmatrix}\begin{Bmatrix}s(0)\\ s(0)\end{Bmatrix} \tag{30}$$

and upon carrying out the partitioned matrix multiplication, we find for $s(t_f)$

$$s(t_f)=\Phi_{ss}s(0)+\Phi_{s\lambda}\lambda(0) \tag{31}$$

which can be solved for λ(0) as

$$\lambda(0)=\Phi_{s\lambda}^{-1}[s(t_f)-\Phi_{ss}s(0)] \tag{32}$$

Equations (32) and (28) allow complete solution of Eq. (25). We are now interested in solving a problem of the same structure, but including the kinematic nonlinearity and using Eq. (32) as starting iteratives for a relaxation procedure, to be described, which will solve this related nonlinear problem.

V. Optimal Control Problem Including Kinematic Nonlinearities

Because of the similarity in structure and in the interest of space conservation, only the key equations will be presented, since this development is analogous to Sec. IV.

The transformed matrix equation of motion (corresponding to Eq. (15)) is

$$\ddot{\mathfrak{t}}+[\Delta^2]\mathfrak{t}=U_T V-\alpha(V^T\dot{\mathfrak{t}})^2[L]\mathfrak{t} \tag{33}$$

where

$$\dot{\theta}=V^T\dot{\mathfrak{t}} \qquad [L]=E^T\begin{bmatrix}0 & 0^T\\ 0 & \mathfrak{M}\end{bmatrix}E$$

and α is a relaxation parameter which controls the participation of the kinematic nonlinearity (centrifugal stiffening) in the differential equation ($\alpha=0$, linear problem of Sec. IV; $\alpha=1$, actual physical value). Defining the state vector, as in Eq. (18), leads to the state equation

$$\dot{s}=A(s)s+BU_T \tag{34}$$

where

$$A(s)=\begin{bmatrix}[0] & [I]\\ [A_{21}(s)] & [0]\end{bmatrix} \qquad A_{21}(s)=-\alpha(V^Ts_2)^2[L]-[\Delta^2]$$

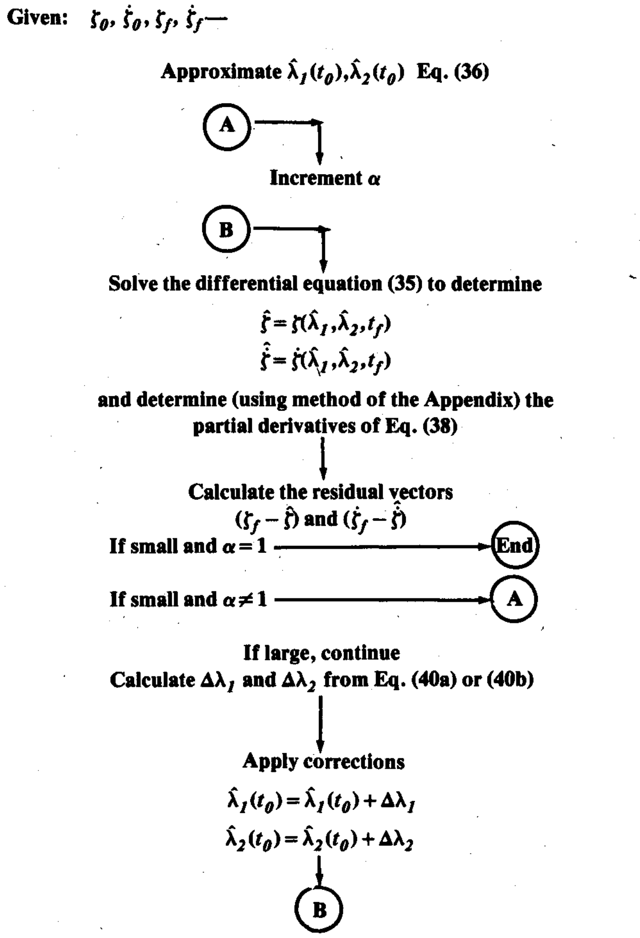

Fig. 3 Differential correction algorithm for determination of initial costate variables.

Defining the optimal control problem as in Sec. IV.A leads to state and costate differential equations which are summarized as:

State Equations

$$\dot{s}=A(s)s-BW_{uu}^{-1}B^T\lambda \tag{35a}$$

Costate Equations

$$\dot{\lambda}=-W_{ss}s-C(s)\lambda \tag{35b}$$

where

$$C(s)=\begin{bmatrix} [0] & A_{21}^T(s) \\ [I] & -2\alpha(V^Ts_2)Vs^T{}_1[L]^T \end{bmatrix}$$

VI. Relaxation Process for the Solution of the Two-Point Boundary-Value Problem

The relaxation parameter α present in Eq. (35) multiplies those terms in which the nonlinearity arises. During the relaxation process α is varied between 0 and 1, with $\alpha=0$ corresponding to the problem solved in Sec. IV and $\alpha=1$ corresponding to the nonlinear equations of motion with the rotational stiffness effect, as presented in Sec. IV. The motivation for introducing the parameter α is that Eq. (35), as does Eq. (25), represents a two-point boundary-value problem with an unknown initial costate. However, as was determined in Sec. IV.B, a closed-form solution for $\alpha=0$ is possible for the initial costates. Now, since the initial costates must be iteratively determined in the nonlinear case, it seems altogether reasonable to try to make use of the costates determined in Sec. IV.B as starting iteratives for the solution of the nonlinear problem. These considerations motivate a successive approximation strategy to solve the two-point boundary-value problem.

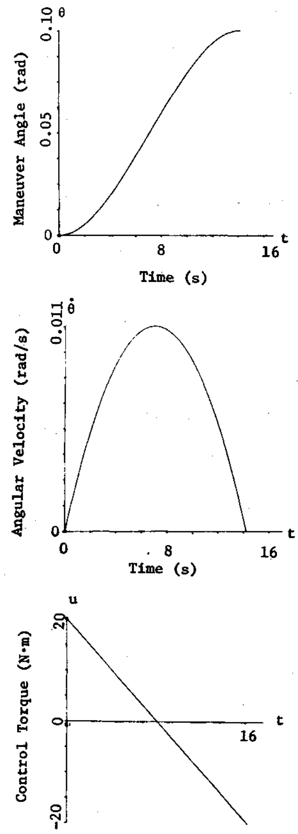

Fig. 4 Case 1 rigid-body rest-to-rest maneuver.

Let approximate initial costates be denoted by

$$\hat{\Lambda}(t_0)=[\hat{\lambda}_1^T(t_0)\hat{\lambda}_2^T(t_0)]^T \qquad \hat{\lambda}_i=[\hat{\lambda}_{i1}\hat{\lambda}_{i2},\ldots,\hat{\lambda}_N] \qquad (i=1,2) \tag{36}$$

We seek correction vectors $\Delta\lambda_1$ and $\Delta\lambda_2$ subject to the terminal constraints

$$\begin{aligned} &\zeta_f-\zeta(\hat{\lambda}_1(t_0)+\Delta\lambda_1,\hat{\lambda}_2(t_0)+\Delta\lambda_2,t_f)=0 \\ &\dot{\zeta}_f-\dot{\zeta}(\hat{\lambda}_1(t_0)+\Delta\lambda_1,\hat{\lambda}_2(t_0)+\Delta\lambda_2,t_f)=0 \end{aligned} \tag{37}$$

In Eq. (37) denoting $\hat{\lambda}_1(t_0)=a$ and $\hat{\lambda}_2(t_0)=b$, and with some specific choice for ζ_0 and $\dot{\zeta}_0$, we let $\hat{\zeta}(a,b,t_f)$ and $\hat{\dot{\zeta}}(a,b,t_f)$ denote the solution of Eqs. (35), (16), and (14). On linearizing Eq. (37), we have

$$\begin{aligned} &\zeta_f-\hat{\zeta}-A_{\zeta\lambda_1}\Delta\lambda_1-A_{\zeta\lambda_2}\Delta\lambda_2=0 \\ &\dot{\zeta}_f-\hat{\dot{\zeta}}-A_{\dot{\zeta}\lambda_1}\Delta\lambda_1-A_{\dot{\zeta}\lambda_2}\Delta\lambda_2=0 \end{aligned} \tag{38}$$

where

$$A_{\zeta\lambda_1}=\left[\frac{\partial\zeta^T}{\partial\lambda_{10}}\Big|_f\right]^T=\left[\frac{\partial(s_1^TE^T)}{\partial\lambda_{10}}\Big|_f\right]^T=E\left[\frac{\partial s_1^T}{\partial\lambda_{10}}\Big|_f\right]^T$$

$$A_{\zeta\lambda_2}=\left[\frac{\partial\zeta^T}{\partial\lambda_{20}}\Big|_f\right]^T=\left[\frac{\partial(s_1^TE^T)}{\partial\lambda_{20}}\Big|_f\right]^T=E\left[\frac{\partial s_1^T}{\partial\lambda_{20}}\Big|_f\right]^T$$

$$A_{\dot{\zeta}\lambda_1}=\left[\frac{\partial\dot{\zeta}^T}{\partial\lambda_{10}}\Big|_f\right]^T=\left[\frac{\partial(s_2^TE^T)}{\partial\lambda_{10}}\Big|_f\right]^T=E\left[\frac{\partial s_2^T}{\partial\lambda_{20}}\Big|_f\right]^T$$

$$A_{\dot{\zeta}\lambda_2}=\left[\frac{\partial\dot{\zeta}^T}{\partial\lambda_{20}}\Big|_f\right]^T=\left[\frac{\partial(s_2^TE^T)}{\partial\lambda_{20}}\Big|_f\right]^T=E\left[\frac{\partial s_2^T}{\partial\lambda_{20}}\Big|_f\right]^T$$

where we have made use of the transformations

$$\zeta = E\mathfrak{t} = Es_1 \qquad \dot{\zeta} = E\dot{\mathfrak{t}} = Es_2$$

Now, defining

$$\Delta\zeta_f = \zeta_f - \hat{\zeta} \qquad \Delta\dot{\zeta}_f = \dot{\zeta}_f - \hat{\dot{\zeta}}$$

and premultiplying the constraint Eq. (38) by $E^T M$ (see Eq. (13)) leads to

$$C_1 = \Phi_{s_1\lambda_1}\Delta\lambda_1 + \Phi_{s_1\lambda_2}\Delta\lambda_2 \qquad C_2 = \Phi_{s_2\lambda_1}\Delta\lambda_1 + \Phi_{s_2\lambda_2}\Delta\lambda_2 \tag{39}$$

where $C_1 = E^T M \Delta\zeta_f$, $C_2 = E^T M \Delta\dot{\zeta}_f$, and $\Phi_{s_1\lambda_1}$, $\Phi_{s_1\lambda_2}$, $\Phi_{s_2\lambda_1}$, $\Phi_{s_2\lambda_2}$ are the corresponding blocks of the state transition matrix for the variables s_1, s_2, λ_1, and λ_2. Now, in order to avoid the possible inconvenience of singular coefficient matrices occurring during the inversion of Eq. (51) for $\Delta\lambda_1$ and $\Delta\lambda_2$, we present two solutions:

Solution 1

$$\Delta\lambda_1 = [\Phi_{s_1\lambda_1} - \Phi_{s_1\lambda_2}\Phi^{-1}_{s_2\lambda_2}\Phi_{s_2\lambda_1}]^{-1}[C_1 - \Phi_{s_1\lambda_2}\Phi^{-1}_{s_2\lambda_2}C_2]$$
$$\Delta\lambda_2 = \Phi^{-1}_{s_2\lambda_2}[C_2 - \Phi_{s_2\lambda_1}\Delta\lambda_1] \tag{40a}$$

Solution 2

$$\Delta\lambda_2 = [\Phi_{s_2\lambda_2} - \Phi_{s_2\lambda_1}\Phi^{-1}_{s_1\lambda_1}\Phi_{s_1\lambda_2}]^{-1}[C_2 - \Phi_{s_2\lambda_1}\Phi^{-1}_{s_1\lambda_1}C_1]$$
$$\Delta\lambda_1 = \Phi^{-1}_{s_1\lambda_1}[C_1 - \Phi_{s_1\lambda_2}\Delta\lambda_2] \tag{40b}$$

The calculation of the partial derivatives is a separate issue, dealt with in the Appendix.

The above discussion can all be summarized as the differential correction algorithm in Fig. 3 for refining given approximate initial costates $\hat{\lambda}_1(t_0)$ and $\hat{\lambda}_2(t_0)$ so that a precise solution to the two-point boundary-value problem is achieved (provided the starting estimates are "sufficiently good").

Let us consider a relaxation process which should effectively guarantee that the algorithm of Fig. 3 will work reliably. The only significant assumption en route to the algorithm was the local linearization of Eq. (37) to obtain Eq. (38). A sequence of α values are introduced and for each α_k, the algorithm of Fig. 3 is integrated using converged costate extrapolations as starting estimates.

Choosing the new value α_{k+1} sufficiently near a previous value α_k (for which a converged solution for $\Lambda_k(t_0) = [\lambda_1^T(t_0), \lambda_2^T(t_0)]_k^T$ has been achieved) provides an adaptive means for maintaining *arbitrarily close* estimates for $\Lambda_{k+1}(t_0)$. Convergence can be accelerated by extrapolating the converged costate behavior for back α values. In our experiments using this approach, we have found that it works efficiently and reliably. Locally singular situations and bifurcations appear possible (where the inverses in both Eqs. (40a) and (40b) fail to exist). In numerous test cases, no singularities have been encountered for the antisymmetric class of maneuvers. A more troublesome issue is the expense associated with calculation of the required state transition matrix. Numerical integration of Eq. (A8) is reliable and *required* for the nonlinear problem, but expensive. Solving for $\Phi(t,0)$, using various eigenvalue/eigenvector algorithms, is much less expensive, but also much less reliable numerically, as well as being limited to the solution of the linear problem presented in Sec. IV.

Also significant is the fact that the costate differential equations typically exhibit weak instability when integrating forward in time. This instability can manifest itself as a computational difficulty if the numerical size of the costates grow to sufficiently large values. This instability is severe for stiff structures, but is typically not as serious for very flexible structures. A number of devices can be employed to circumvent this problem, including various iterative algorithms which iterate on $\Lambda(t_f)$ instead of $\Lambda(t_0)$, and solve the costate differential equations backward in time. This difficulty did not prove severe in the calculations of this paper, so it was not necessary to introduce alternative iteration processes.

VII. Applications to Example Maneuvers

Several example maneuvers have been determined using the above formulations. For all cases, we have assumed the geometry of Fig. 1 with the following configuration parameters: the inertia of the undeformed structure, J, is 7000 kg-m^2; the mass/unit length of the four identical appendages, ρ, is 0.0004 kg/m; the length of each cantilevered appendage, L, is 150 m; and the flexural rigidity of the flexible members, EI, is 1500 kgm/s^2 for cases 2-4 (Table 1).

The diameter of the hub was neglected in comparison to the appendage length. In Eq. (5), we adopt as assumed modes the admissible functions

$$\phi_r = (x/L)^{r+1} \qquad (r = 1,2,\ldots,\infty) \tag{41}$$

which obviously satisfy the geometric boundary conditions of a clamped-free appendage.

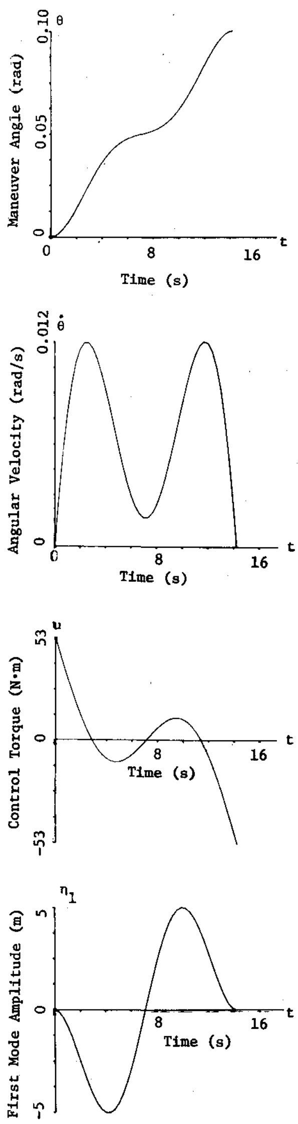

Fig. 5 Case 2L, 2N flexible appendages rest-to-rest maneuver $t_f = 2\pi/\omega_1$.

Table 1 Description of test case maneuvers

Case No.	Qualitative description	No. of modes N	θ_0, rad	$\dot{\theta}_0$, rad/s	θ_f, rad	$\dot{\theta}_f$, rad/s	W_{uu}	W_{ss}
1	Rigid appendages Rest-to-rest maneuver $t_f = 14.221$ s	0	0	0	0.1	0	1.0	[0]
2L	Linear kinematics Rest-to-rest maneuver $t_f = 2\pi/\omega_1 = 14.221$ s	1	0	0	0.1	0	1.0	[I]
2N	Nonlinear kinematics Rest-to-rest maneuver $t_f = 2\pi/\omega_1 = 14.221$ s	1	0	0	0.1	0	1.0	[I]
3L	Linear kinematics Spinup maneuver $t_f = 60$ s	2	0	0	2π	0.5	1.0	[I]
3N	Nonlinear kinematics Spinup maneuver $t_f = 60$ s	2	0	0	2π	0.5	1.0	[I]
4L	Linear kinematics Rest-to-rest maneuver $t_f = 60$ s	4	0	0	π	0	1.0	[I]
4N	Nonlinear kinematics Rest-to-rest maneuver $t_f = 60$ s	4	0	0	π	0	1.0	[I]

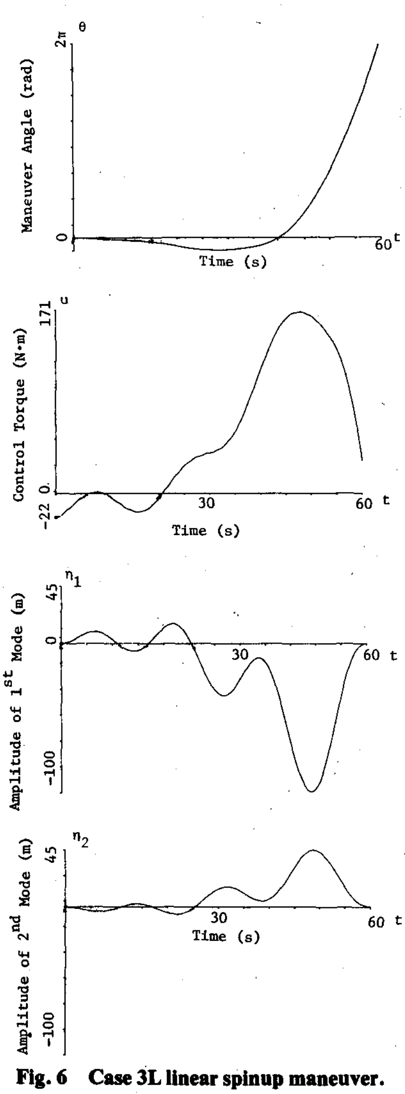

Fig. 6 Case 3L linear spinup maneuver.

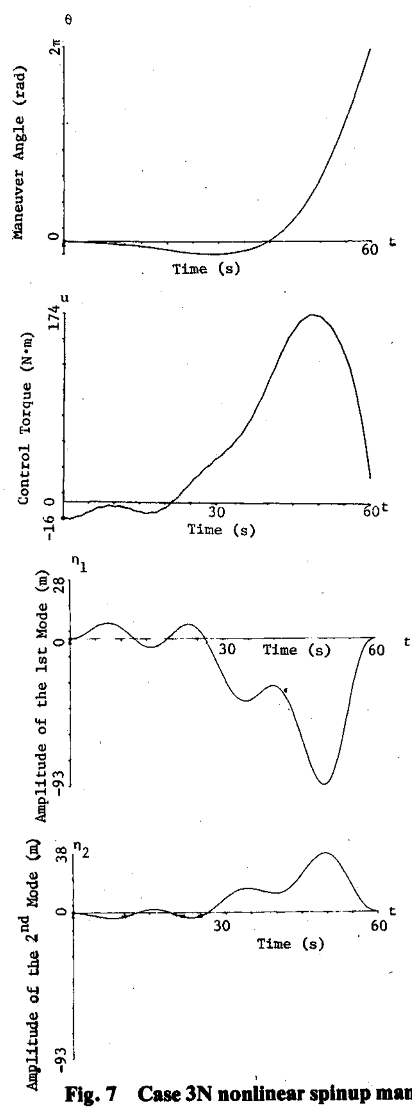

Fig. 7 Case 3N nonlinear spinup maneuver.

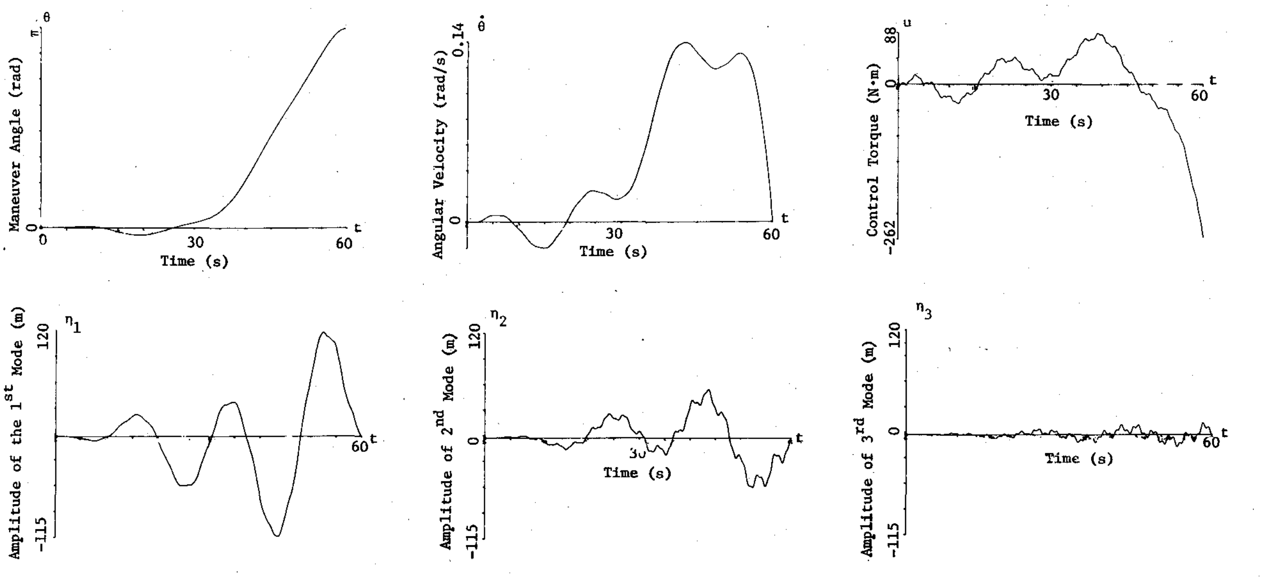

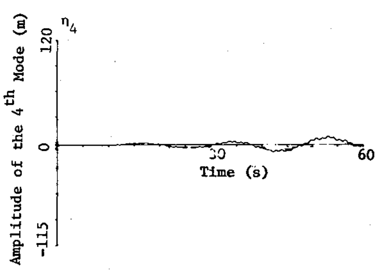

Fig. 8 Case 4L rest-to-rest maneuver controlling and arresting four modes.

With reference to Table 1, we considered maneuvers using seven models for the system dynamics with $N=0$, 1, 2, and 4 assumed modes; and for the flexible cases, either deleting ($\alpha=0$) or including ($\alpha=1$), the nonlinear coupling term in equations of motion Eq. (34). For the nonlinear cases, the two-point boundary-value problem was solved by relaxing α from zero to unity with a finite number of intermediate values (the largest number of relaxation steps was five, required for case 3N). For each α value, costate estimates were extrapolated from the converged neighboring solutions, the algorithm of Fig. 3 reliably converged in at most three differential corrections.

Now, with reference to Table 1 and Figs. 4-7, we consider qualitatively the graphical summaries of the state and control histories along the maneuvers calculated.

Note that for case 2L, the torque required (Fig. 5c to carry out the rigid rotation and arrest the terminal amplitude and velocity of the first mode) is antisymmetric and oscillates about the straight line torque of Fig. 4c for the rigid case. The antisymmetric torque history is a direct consequence of the fact that the specified final time is equal to the period of the first mode and the rest-to-rest boundary conditions. As is evident in all subsequent cases, the torque history is generally asymmetric. Also significant is the fact that the linear (case 2L) and nonlinear solutions (case 2N) were identical to plotting accuracy, slight numerical variations occurred in the fourth significant digit of the state variables. Also controlled, but not displayed, was the time derivatives of the modal amplitudes; in all cases, they had terminal values of 10^{-7} or smaller.

Cases 3L and 3N are a most interesting spinup case. The somewhat counter-intuitive initial reverse torque (Figs. 6b and 7b) and corresponding body rotation (Figs. 6a and 7a) is required to set up vibratory motion, which can be most efficiently arrested in conjunction with an eventual 360-deg rotation and matching of uniform angular velocity of 0.5 rad/s. This "reversal" is typical of fixed final time maneuvers with final angular velocity above a critical value.[11] In this case, the nonlinear term contributed significantly to the motion and torque history (note the shape changes and, especially, the scale changes, between Figs. 6 and 7).

Cases 4L and 4N (Figs. 8a-g—for brevity, we do not show case 4N variables) demonstrate the capability of the fomulation to simultaneously control and arrest several (four) modes and accomplish a large rotational maneuver (180 deg). It is significant that this case (with much smaller maximum angular velocity than case 3), the linear solutions vibration amplitudes were about 10% greater than the nonlinear solution (due to centrifugal stiffening), but even for these very large amplitudes, the motion is qualitatively the same (two-digit agreement was achieved throughout most of the maneuver). This leads one to conclude that, in applications, "slow" maneuvers of this configuration may require only linear coupling between structural and rotational degrees of freedom. Although these large deflections likely exceed the validity of the model; they do demonstrate that the formulation is valid.

VIII. Concluding Remarks

The results of this paper provide a basis for systematic solution for optimal large-angle single-axis spacecraft rotational maneuvers. A method is proposed and demonstrated for solving the nonlinear two-point boundary-value problems of attitude dynamics.

Appendix: Computation of State and Costate Partial Derivatives

Referring to Eq. (38) and subsequent developments in the text of this paper, we need the four partial derivative matrices

$$\Phi_{s_i\lambda_j} = \left[\frac{\partial s_i^T}{\partial \lambda_{j0}} \bigg|_f \right]^T \qquad (i,j=1,2)$$

To determine these partial derivatives, we first consider the state vector s defined by

$$s = [s_1^T(t) \quad s_2^T(t) \quad \lambda_1^T(t) \quad \lambda_2^T(t)]^T \tag{A1}$$

Next, assuming that the time derivative of s is known to be

$$\dot{s} = F(s,t) \tag{A2}$$

we are lead to the formal solution for s:

$$s(t) = s(t_0) + \int_{t_0}^{t_f} F(s(\tau),\tau)\,\mathrm{d}\tau \tag{A3}$$

Taking the partial derivatives of Eq. (A3) with respect to $s(t_0)$, we obtain

$$\left[\frac{\partial s(t)}{\partial s(t_0)}\right] = [I] + \int_{t_0}^{t_f} \left[\frac{F(s(\tau),\tau)}{\partial s(\tau)}\right]\left[\frac{\partial s(\tau)}{\partial s(t_0)}\right]\mathrm{d}\tau \tag{A4}$$

From Eq. (A4), we conclude that the initial conditions for $\partial s(t)/\partial s(t_0)$ are given by

$$\left[\frac{\partial s(t)}{\partial s(t_0)}\bigg|_{t=t_0}\right] = [I] \tag{A5}$$

On taking the time derivative of Eq. (A4), we obtain

$$\frac{\mathrm{d}}{\mathrm{d}t}\left[\frac{\partial s(t)}{\partial s(t_0)}\right] = \left[\frac{F(s(t),t)}{\partial s(t)}\right]\left[\frac{\partial s(t)}{\partial s(t_0)}\right] \tag{A6}$$

or defining

$$\Phi(t,t_0) = \left[\frac{\partial s(t)}{\partial s(t_0)}\right] \text{ (the state transition matrix)} \tag{A7}$$

Eq. (A6) becomes

$$\dot{\Phi} = \mathfrak{F}\Phi \qquad \mathfrak{F} = \left[\frac{\partial F(s(t),t)}{\partial s(t)}\right] \tag{A8}$$

By integration of Eqs. (A2) and (A8), subject to Eq. (A5), from $t=t_0$ to $t=t_f$, we obtain the partials of the current state $s(t_f)$ with respect to the initial state $s(t_0)$. The matrices $\Phi_{s_1\lambda_1}$, $\Phi_{s_1\lambda_2}$, $\Phi_{s_2\lambda_1}$, and $\Phi_{s\lambda_2}$ are obtained from $\Phi(t_f, t_0)$,

$$\underset{24\times 24}{\Phi(t_f,t_0)} = \begin{bmatrix} \Phi_{s_1s_1}(t_f,t_0) & \Phi_{s_1s_2}(t_f,t_0) & \Phi_{s_1\lambda_1}(t_f,t_0) & \Phi_{s_1\lambda_2}(t_f,t_0) \\ \Phi_{s_2s_1}(t_f,t_0) & \Phi_{s_2s_2}(t_f,t_0) & \Phi_{s_2\lambda_1}(t_f,t_0) & \Phi_{s_2\lambda_2}(t_f,t_0) \\ \Phi_{\lambda_1s_1}(t_f,t_0) & \Phi_{\lambda_1s_2}(t_f,t_0) & \Phi_{\lambda_1\lambda_1}(t_f,t_0) & \Phi_{\lambda_1\lambda_2}(t_f,t_0) \\ \Phi_{\lambda_2s_1}(t_f,t_0) & \Phi_{\lambda_2s_2}(t_f,t_0) & \Phi_{\lambda_2\lambda_1}(t_f,t_0) & \Phi_{\lambda_2\lambda_2}(t_f,t_0) \end{bmatrix}$$

and where the above dimensions assume that five modes are used in the approximation.

With the results above, we can proceed with the processes defined in Secs. IV and V.

References

[1] Likins, P.W., Barbera, F.J., and Baddeley, V., "Mathematical Modeling of Spinning Elastic Bodies for Modal Analysis," *AIAA Journal,* Vol. 11, Sept. 1973, pp. 1251-1258.

[2] Meirovitch, L., "A Stationary Principle for the Eigenvalue Problem for Rotating Structures," *AIAA Journal,* Vol. 14, Oct. 1976, pp. 1387-1394.

[3] Junkins, J.L. and Turner, J.D., "Optimal Continuous Torque Attitude Maneuvers," Paper 78-1400, presented at the AIAA/AAS Astrodynamics Conference, Palo Alto, Calif., Aug. 1978.

[4] Breakwell, J.A., "Optimal Feedback Maneuvering of a Flexible Spacecraft," AAS Preprint 79-157, presented at the AAS/AIAA Astrodynamics Conference, June 1979.

[5] Meirovitch, L., *Methods of Analytical Dynamics,* McGraw-Hill Book Co., New York, 1970, p. 68.

[6] Bryson, A.E. and Ho, Y.C., *Applied Optimal Control,* John Wiley & Sons, Inc., New York, 1975, Chaps. 2 and 5.

[7] Young, Y.C., *Calculus of Variations and Optimal Control Theory,* W.B. Saunders, Co., Philadelphia, pp. 308-321.

[8] Leitmann, G., *Optimization Techniques With Applications to Aerospace Systems,* Academic Press, New York, 1962, Chap. 7 (R.E. Kopp's contribution).

[9] Pontryagin, L.S., et al., *The Mathematical Theory of Optimal Processes,* Interscience, London, 1962.

[10] Kirk, D.E., *Optimal Control Theory. An Introduction,* Prentice Hall, New Jersey, 1970.

[11] Turner, J.D., "Optimal Continuous Torque Attitude Maneuvers for Flexible Spacecraft," Ph.D. Dissertation, Virginia Polytechnic Institute & State University, Blacksburg, Va., 1980.